RT-RPA-Cas12a-based discrimination of SARS-CoV-2 variants of concern

Guiyue Tang[1,#], Zilong Zhang[2,#], Wei Tan[1,#], Fei Long[1], Jingxian Sun[1], Yingying Li[1], Siwei Zou[1], Yujiao Yang[3,4], Kezhu Cai[1,5], Shenwei Li[2], Zhiyi Wang[2], Jiakun Liu[1], Guobing Mao[1], Yingxin Ma[1], Guo-Ping Zhao[1,3,4,6,*], Zhen-Gan Tian[2,*], Wei Zhao[1,*]

[1]CAS Key Laboratory of Quantitative Engineering Biology, Shenzhen Institute of Synthetic Biology, Shenzhen Institutes of Advanced Technology, Chinese Academy of Sciences, Shenzhen 518055, China;

[2]Shanghai International Travel Healthcare Center, Shanghai Customs District P. R. China, Shanghai 200335, China;

[3]CAS Key Laboratory of Synthetic Biology, CAS Center for Excellence in Molecular Plant Sciences, Chinese Academy of Sciences, Shanghai 200032, China;

[4]CAS Key Laboratory of Synthetic Biology, University of Chinese Academy of Sciences, Beijing 100049, China;

[5]School of Engineering, Southern University of Science and Technology, Shenzhen 518055, China;

[6]State Key Lab of Genetic Engineering & Institutes of Biomedical Sciences, Department of Microbiology and Microbial Engineering, School of Life Sciences, Fudan University, Shanghai 200433, China;

[#]These authors contributed equally.

[*]To whom correspondence should be addressed: wei.zhao1@siat.ac.cn, tianzhenganciq@163.com, and gpzhao@sibs.ac.cn.

Abstract

Timely and accurate detection of SARS-CoV-2 variants of concern (VOCs) is urgently needed for pandemic surveillance and control. However, current methods are limited by the low sensitivity, long turn-around time or high cost. Here, we report a nucleic acid testing-based method aiming to detect and discriminate SARS-CoV-2 VOCs by combining RT-RPA and CRISPR-Cas12a detecting assays (RRCd). With a detection limit of 10 copies RNA/reaction, RRCd was validated in 204 clinical samples, showing 99% positive predictive agreement and 100% negative predictive agreement, respectively. Critically, using specific crRNAs, representatives of single nucleotide polymorphisms and small deletions in SARS-CoV-2 VOCs including N501Y, T478K and ΔH69-V70 were discriminated by RRCd, demonstrating 100% accuracy in clinical samples with $C_t < 33$. The method completes within 65 min and could offer visible results without using any electrical devices, which may facilitate point-of-care testing of SARS-CoV-2 and its variants.

Keywords

SARS-CoV-2, variant of concern, RRCd, point-of-care testing, CRISPR

Introduction

The pandemic of COVID-19 has caused 494.5 million infections and 6.1 million deaths as of April 10th 2022 (https://covid19.who.int/table). The pathogen of this pandemic, SARS-CoV-2, has undergone rapid and constant mutations in the process of transmissions, bringing worldwide uncertainty to the diagnostics, vaccine effectiveness and therapeutics (Tao et al. 2021).

Since November 2020, generally five rapidly expanding SARS-CoV-2 lineages have been discovered and designated as variants of concern (VOCs), *i.e.*, the Alpha, Beta, Gamma, Delta, and Omicron (Oude Munnink et al. 2021) (**Supplementary Figure 1**). Besides the current Omicron, among these lineages, the Alpha and Delta VOCs were dominant in frequency over a relatively long period of time. With gradual resumption of air travel, Customs, and ports, certain previously isolated areas were riskily exposed to the SARS-CoV-2 variants. These variants, either with higher infectivity or increased pathogenicity, could trigger multiple outbreak waves unless they are detected timely and accurately (Tao et al. 2021, Oude Munnink et al. 2021).

Although quantitative reverse transcription PCR (RT-qPCR) performs as a gold standard for the SARS-CoV-2 detection, it is barely used to genotype the SARS-CoV-2 VOCs due to the limitations as an amplicon-based method. The current method is heavily based on in-depth whole-genome sequencing, which not only relies on bulk instruments and trained personnel but is also time-consuming and with relatively high cost (Crits-Christoph et al. 2021, Kumar et al. 2021). A recent study showed that the multiplex qPCR could discriminate some SARS-CoV-2 VOCs by targeting specific small deletions(Vogels et al. 2021). However, this method is insensitive to the key point mutations and other developing variations in SARS-CoV-2. Similarly, antigen-based detection assays have lower sensitivity than

RT-qPCR and have not yet been reported to identify SARS-CoV-2 VOCs (Peto and Team 2021).

CRISPR-based technology was proven to have unique advantages in molecular diagnosis over the conventional PCR methods in terms of specificity and operability (Chen et al. 2018, Joung et al. 2020, Fozouni et al. 2021). Two CRISPR-based COVID-19 diagnostic methods, DETECTR and SHERLOCK, have been developed using either Cas12a or Cas13a, with the characteristics of rapid, ultrasensitive and easy-to-implement (Broughton et al. 2020, Patchsung et al. 2020). Moreover, CRISPR assays such as RAY were employed to identify the point mutations in SARS-CoV-2 due to the high specificity of Cas/guide-RNA recognition (Kumar et al. 2021, Wang et al. 2021). Nevertheless, the relying on well-designed ligation probes somehow limited the targeting capability to diverse mutation sites. Recently, CRISPR-based point-of-care tests (POCT) of SARS-CoV-2 were reported (de Puig et al. 2021, Teng et al. 2019). The methods provided visual readout using minimal fluorescent instruments and could identify multiple SARS-CoV-2 VOCs, among the synthetic samples though. Hence, significant efforts are still needed in respect to improving the detection sensitivity and validating the methods with clinical samples.

Here, we report a method combining reverse transcription-recombinase polymerase amplification (RT-RPA) and CRISPR-Cas12a technology based on our HOLMES test platform (Li, Cheng, Liu, et al. 2018, Li, Cheng, Wang, et al. 2018), aiming to detect and discriminate SARS-CoV-2 VOCs. By exchanging the crRNA sequences, the method (RRCd) achieved to discriminate the well-known single nucleotide polymorphisms (SNPs) of N501Y and T478K as well as the small deletion of ΔH69-V70, corresponding to the major VOCs worldwide. RRCd was validated in 204 clinical samples after being systematic optimization, showing 99% positive

predictive agreement and 100% negative predictive agreement, respectively. The results of RRCd could be visualized within about one hour. Moreover, all procedures including the sample lysis were able to carry out at 37 °C and with no needs for RNA extraction and purification, which is very conducive to the development of POCT products.

Results

Technical route of RRCd assay

The CRISPR-*Lb*Cas12a-based nucleic acid test platform HOLMES (Li, Cheng, Wang, et al. 2018) was chosen as the starting core to design the technical route for RRCd (**Figure 1, Supplementary Figure 2**). We conduct a two-step RT-RPA amplification on SARS-CoV-2 genes to provide adequate double-stranded DNA (dsDNA) for the following CRISPR recognition system (**Figure 1, II**). By designing specific crRNA, Cas12a recognizes and *cis*-cleaves the dsDNA templates of SARS-CoV-2 or its variants. Meanwhile, the formation of the ternary complex of Cas12a-crRNA-dsDNA activates the *trans*-activity of Cas12a, which leads to the cleavage of the non-targeted single-stranded DNA (ssDNA) probe in the system (**Figure 1, III**). The results could be quantified directly by fluorescence detection of the fluorophore-quencher ssDNA (FQ-ssDNA) (**Figure 1, IIIa**) or captured by lateral-flow strip using the FITC-Biotin ssDNA (FB-ssDNA) (**Figure 1, IIIb**).

Hence, different from the previous methods (Broughton et al. 2020, Patchsung et al. 2020, Ding et al. 2020), RRCd combines the advantages of high sensitivity of RT-RPA (Lobato and O'Sullivan 2018) and high specificity of CRISPR-Cas12a (Chen et al. 2018) (**Table 1**). In comparison with Cas9 and Cas13, Cas12a in RRCd

possesses greater specificity and lower mismatch tolerance (Chen et al. 2018), making it more suitable for SARS-CoV-2 VOCs genotyping.

The specificity analyses of RRCd assay

Representative mutations in spike (S) protein were used for genotyping of the SARS-CoV-2 lineages (Munnink et al. 2021) (**Figure 2A**). By screening optimal RT-RPA primers (**Supplementary Figure 3**) and crRNAs (**Supplementary Figure 4**) that target to the S protein encoding gene, RRCd was readily applied for the detection and discrimination of SARS-CoV-2 VOCs (**Figure 2B-G**). These VOCs include the first reported Alpha and Beta mutation N501Y (Tegally et al. 2021) (**Figure 2B, C**), the recent reported T478K mutation in Delta and Omicron VOCs (Kumar et al. 2022) (**Figure 2D, E**), and the small deletions such as ΔH69-V70 in Alpha and Omicron VOCs (Meng et al. 2021) (**Figure 2F, G**). The N501Y mutation in the receptor-binding domain (RBD) of S protein was reported to cause an increased transmission and infectivity of SARS-CoV-2 (Liu et al. 2022). The T478K nutation in the RBD is also involved in higher transmissibility by the increased affinity to human ACE2 receptor (Kumar et al. 2022), while the deletion of H69V70 at the N-terminal domain is shown to allow the virus to replicate more efficiently (Meng et al. 2021).

Our test results were demonstrated by both the fluorescence-based and lateral-flow readouts, representing the *trans*-cleavage activity of Cas12a (Chen et al. 2018, Li, Cheng, Liu, et al. 2018) (**Figure 2B-G**). Additionally, we confirmed this specific cleavage using polyacrylamide gel electrophoresis analyses by leveraging of the Cas12a *cis*-cleavage activity (Chen et al. 2018) (**Figure 2H-J**). Moreover, RRCd can be used for the discrimination of SARS-CoV-2 from other phylogenetic related viruses (**Supplementary Figure 5**).

142

143 **The detection limit of RRCd**

144 To determine the limit of detection (LoD) of RRCd, we built a standard curve to
145 dissect the correspondences between the viral copy numbers and the C_t values using
146 SARS-CoV-2 pseudovirus (**Supplementary Figure 6**). The C_t values of each dilution
147 were measured using RT-qPCR targeting *N* gene or *ORF1ab* gene to mimic the
148 clinical C_t ranges. Despite showing distinct kinetics, the fluorescence-based readouts
149 revealed that the LoDs of all the targeted regions (*E* gene, N501, Y501, T478, and
150 K478 of *S* gene) were ~10 copies per reactions, corresponding to a C_t value of 35 in
151 the RT-qPCR assay (**Figure 3**). The fluorescence results from a 30-min CRISPR
152 reaction suggested that the detection sensitivity of N501 is a slightly higher than that
153 of Y501 (**Figure 3B, C**), while the detection sensitivity of T478 is a slightly lower
154 than that of K478 (**Figure 3D, E**). It is worth noting that the detection sensitivity of
155 the lateral-flow readouts is about 10-folds lower than that of the fluorescence-based
156 readouts (**Figure 3**). The detection of Y501 and K478 was shown to be the most
157 sensitive when using the lateral-flow readout, with the LoDs of ~10 copies per
158 reactions (**Figure 3C, E**).

159 To avoid false-discriminative results, we further assessed the factors that may
160 affect the detection sensitivity in RRCd, including the sample volume and probe
161 inputs, the usage of RNase H, T4 gene 32 protein, Bsu DNA polymerase, RPA kits,
162 and Mg^{2+}. We found the sample volume and the usage of T4 gene 32 protein (Villalva
163 et al. 2001) are the key factors affecting RRCd sensitivity mostly (**Supplementary**
164 **Figure 7**).

165

166

Validation of RRCd in detection and discrimination of clinical samples

Based on the optimized procedures, we evaluated the performance of RRCd on detecting COVID-19 clinical samples isolated from nasopharyngeal and salivary swabs. In coordination with the scenario of POCT, our available samples were collected from Shanghai Customs where the susceptible patients were characterized as asymptomatic and with low virus load (**Supplementary Figure 8**). To minimize the cognitive bias, all information of the clinical samples was confidential to study staff before the detection.

A validation study of SARS-CoV-2 detection was conducted on a total of 96 clinical samples (54 RT-qPCR-verified positive samples and 42 RT-qPCR-verified negative samples). Both *E* gene and *S* gene were used as the targeted sequences to acquire the double-checked detection results (**Figure 4, Supplementary Figure 9**). RRCd identified all the positive samples with $C_t < 33$ through both lateral-flow and fluorescence-based readouts. In addition, 42 COVID-19 negative samples were all identified without false positive results from both readouts. Samples beyond the C_t value of 32 were more likely to be detected by targeting the *E* gene ($C_t \leq 35$, 100% detected) than the *S* gene (**Figure 4**). The detection sensitivity of these results was comparable to the RT-LAMP-Cas12 based DETECTR (Broughton et al. 2020) and the RT-RPA-Cas13 based SHERLOCK (Patchsung et al. 2020), showing a 99% positive predictive agreement (PPA) and 100% negative predictive agreement (NPA) in both readouts ($C_t < 33$) (**Table 2**).

We next evaluated the performance of RRCd on discrimination of SARS-CoV-2 VOCs. The 501 position of *S* gene was used as a target to detect SARS-CoV-2 VOCs, such as the Alpha, Beta, Gamma, and Omicron (Tegally et al. 2021). A total of 68 clinical samples, consisting of 28 genome-sequencing-verified N501 samples and 19

genome-sequencing-verified Y501 samples, were collected from March 3rd to April 10th 2021 at Shanghai Customs. RRCd discriminated all the variants from samples with a $C_t < 32$, either using lateral-flow readouts or fluorescence-based readouts (**Figure 5A, Supplementary Figure 10**). However, the discrimination ability decreased strikingly when testing the samples with C_t values beyond 33, which is possibly due to the relatively high LoD of *S* gene 501 as mentioned above (**Figure 3**).

The 478 position of *S* gene could be used as a target to identify Delta and Omicron VOCs (**Figure 5B, Supplementary Figure 11**). A total of 40 clinical positive samples, consisting of 7 genome-sequencing-verified T478 samples and 14 genome-sequencing-verified K478 samples, were collected from May 27th and October 29th 2021. RRCd was able to discriminate all the variants targeting the *S* gene 478. Moreover, RRCd displayed a relatively higher sensitivity in detecting the position of 478 than that of 501, with the C_t value reaching 34. Although using a relatively small sample group, the detection results were confirmed by both readouts with 0% false-discriminant rates (**Figure 5B**). Taken together, these clinical data suggested that RRCd was able to detect and discriminate the SARS-CoV-2 VOCs, accurately and sensitively (**Table 2**).

Discussion

Although a decreased lethality of the circulating Omicron has been reported, its overall mortality rate has not dropped because its dramatically increased infectivity (Nyberg et al. 2022). The frequent outbreak waves of COVID-19 highlight the needs for detection methods that are rapid, sensitive, and specific. However, the current method relying on deep genome sequencing is limited by the high cost, long turn-around time, and the reduced overall sensitivity (Kumar et al. 2021). Although

the recently developed CRISPR-based methods were characterized as sensitive and easy-to-implement, most of them were barely validated by the large clinical samples or have a limited adaptability (Wang et al. 2021, Teng et al. 2019, de Puig et al. 2021).

In the present study, RRCd completed in ~1 hour and displayed a sensitivity down to 10 copies per reaction. By targeting and identifying the representative N501Y, T478K and ΔH69-V70 mutations, RRCd discriminated COVID-19 samples of Alpha, Delta, and Omicron VOCs. The method was validated in 204 clinical COVID-19 samples, with 99% PPA and 100% NPA for the samples of $C_t < 33$ through both the fluorescence and the lateral-flow readouts (**Table 2**). Moreover, The SARS-CoV-2 detection by direct lysing the clinic samples without RNA extraction and purification was demonstrated (**Supplementary Figure 12**). Although a relatively small sample size was used, these results indicated that the whole process of RRCd including the RT-RPA amplification and the lateral-flow detection is independent of electrical devices, which may facilitate the development of POCT products (**Table 1**).

In addition, the RRCd assay has the potential to be easily adapted to detect novel mutations on SARS-CoV-2 or other viruses by designing the new RT-RPA primers and crRNAs, without changing the subsequent detection procedures and ssDNA probes (**Figure 1, Supplementary Figure 2**). Overall, RRCd can be performed in sites with few detection equipment (*e.g.*, self-testing) or limited power access (*e.g.*, underdeveloped areas), or situations when quick turnaround times are needed (*e.g.*, hospital emergency). Nevertheless, the POCT products for RRCd needs to be further investigated.

Materials and methods

Clinical sample collection and ethics statement

All 204 nasopharyngeal and salivary samples were collected at Shanghai International Travel Healthcare Center (SITHC), Shanghai Customs District P. R. China, from March 3rd and to October 29th 2021. The samples were treated in strict accordance with WHO recommended standard operation procedure. Ethical approval of the study was given by the Bioethics Committee of Bio-X Institute of Shanghai Jiao Tong University (COA: M202007).

RT-qPCR for the SARS-CoV-2 detection

The viral RNA of each swab was extracted and purified from a 200 µl-swab transport media using an automatic nucleic acid platform (SSNP-3000A, Bioperfectus tech., China) according to the manufacturer's instruction. A 100 µl RNase-free water was used to elute the RNA. Viral lysis and RNA extraction were performed in a biosafety level 3 laboratory, whereas other procedures were performed in a biosafety level 2 laboratory.

The quantitative reverse transcription PCR (RT-qPCR) for SARS-CoV-2 detection was performed with a 2019-nCoV nucleic acid detection kit (BioGerm, Shanghai, China) according to the manufacturer's protocol. Each RT-qPCR reaction had a final volume of 25 µl, including 5 µl purified RNA, 12 µl reaction buffer, 4 µl enzyme solution and 4 µl probe primers solution. RT-qPCR assay was performed on QuantStudio Dx Real-Time PCR (Applied Biosystems, MA, USA) under the following conditions: incubation at 50 °C for 15 min and 95 °C for 5 min, 45 cycles of denaturation at 94 °C for 15 s, and extension and fluorescence signal reading at 55 °C for 45 s. Two target genes, *i.e.*, the *ORF1ab* gene and the *N* gene, were

simultaneously amplified and tested in the RT-qPCR assay. The test result was deemed as positive when the cycle threshold values (C_t value) of both *ORF1ab* and *N* genes $\leq$ 38; otherwise, a negative result was deemed. These diagnostic criteria were based on the recommendation from the National Institute for Viral Disease Control and Prevention (China) (http://ivdc.chinacdc.cn/kyjz/202001/t20200121_211337.html).

Design and screening of the RT-RPA primers and crRNAs

For the detection of SARS-CoV-2, *E* gene was selected as the test target using the RT-RPA primers and crRNA recommended by WHO with minor modifications (**Supplementary Table 1**).

For the detection of SARS-CoV-2 VOCs, the representative mutations in the *S* gene were selected as the test targets. Aiming to distinguish the most prevailing SARS-CoV-2 VOCs (*i.e.*, the Alpha, Delta, and Omicron), we designed the RT-RPA primers on the conserved regions flanking the mutations of *S* gene 478 and 501 (**Supplementary Table 1**), respectively, and screened the best pairs by agarose gel analyses for the amplification efficiency of dsDNA. Two pairs of optimal RT-RPA primers (S501RPAF1/S501RPAR1 and S478RPAF3/S478RPAR5) were selected for the detection of *S* gene 478 and 501, respectively. To further evaluate their applicability in the detection of clinical samples, these RT-RPA primers were aligned with 859,132 full-length SARS-CoV-2 genome sequences collected from January 1st 2021 to December 31th 2021 in the GISAID database (Buch et al. 2011). The results showed that these pairs of RT-RPA primers hit 99.7% of the genome sequences, demonstrating a good applicability in detection of prevailing clinical samples.

Optimal crRNAs for the discrimination of *S* gene 501 variants were assessed

by determining the specificity of the crRNA to the single-base mismatched *S* gene templates. DNA fragments containing wild-type *S* gene 501 with point mutations were synthesized in pUC19 backbone plasmid by Sangon Biotech. These *S* gene 501 regions were transcribed into RNA using HiScribe T7 High Yield RNA Synthesis kit (Cat# E2050S, New England Biolabs) at 37 °C for 4 h, whose products were further analyzed using both fluorescence-based and lateral-flow readouts. The crRNA-N501 was employed to discriminate the single-base mismatches. Based on this approach, we designed the crRNAs for the discrimination of other SARS-CoV-2 VOCs. All crRNA and RT-RPA primer sequences used in this study are listed in **Supplementary Table 1**.

crRNA generation

The DNA templates (**Supplementary Table 1**) for *in vitro* transcription (IVT) of crRNAs were designed with T7 primer binding sites using CRISPR-RT Design Tool (http://bioinfolab.miamioh.edu/CRISPR-RT) and synthesized by Sangon Biotech (Shanghai, China). The crRNAs were transcribed using HiScribe T7 High Yield RNA Synthesis kit (Cat# E2050S, New England Biolabs) at 37 °C for 16 h. Then, the crRNAs were purified using RNA Clean and Concentrator kit (Cat# R1017, Zymo Research). The concentration of crRNA was quantified by NanoDrop 2000C spectrophotometer (Thermo Scientific) and stored at -80 °C before use.

Reverse transcription and recombinase polymerase amplification (RT-RPA)

A 20 µl volume-basic RT reaction mixture was used with 1 × RT buffer (Cat# EP0442, Thermo Scientific), 10 µl RNA template, 200 U RevertAid reverse transcriptase (Cat# EP0442, Thermo Scientific), 1.25 µM RT-RPA forward and

reverse primer mix, 1 mM dNTP mix (Cat# P031-01, Vazyme, Nanjing, China), and 20 U RNase inhibitor (Cat# N8080119, Thermo Scientific). The RT reaction mixture was incubated at 37 °C for 15 min to generate cDNA. Then, a 10 µl RT product was transferred into the 50 µl-basic RPA reaction mixture, which contains 29.5 µl rehydration buffer, one freeze-dried RPA reaction pellet (Cat# TABAS03KIT, TwistDx), 0.5 µM RT-RPA forward and reverse primer mix, and 14 mM MgOAc (last added to initiate the reaction). The RPA reaction mixture was incubated at 37 °C for another 15 min. The RNA extracts from SARS-CoV-2 pseudovirus and the RNase-free water were used as the positive control (PC) and negative control (NC), respectively.

CRISPR *trans*-cleavage assay for fluorescence-based and lateral-flow readouts

Briefly, a 100 µl volume basic CRISPR reaction mixture was used with 1 × *Lba*Cas12a buffer, 5 µl RT-RPA product, 0.2 µM *Lba*Cas12a (Cat# M0653T, New England Biolabs), 0.6 µM crRNA, 10 µM $MgCl_2$, 10 nM fluorophore (FAM)-quencher (BHQ1) ssDNA probe (FQ-ssDNA, Sangon Biotech) for the fluorescence-based detection, or 50 nM FTIC-Biotin ssDNA probe (FB-ssDNA, Zoonbio Biotechnology, Nanjing, China) for the lateral flow-based detection.

For the fluorescence-based readout, a 96-well plate containing 100 µl reaction mixture was incubated at 37 °C using the Cytation 5 Mul-Mode Reader (BioTek, VT, USA). Usually, a 60-min monitoring was used with an interval time of 30 s. The fluorescence excitation and emission wavelength were set as 485 nm and 520 nm, respectively. The relative fluorescence intensity (F/F_0) was calculated as the fluorescence signal relative to the starting signal. Generally, the fluorescence signals at the 30 min-reactions were quantified as F_{30}/F_0. In this study, $(F_{30}/F_0)_{Sample}$ /

339 $(F_{30}/F_0)_{NC} \geq 1.2$ indicates the positive result while $(F_{30}/F_0)_{Sample} / (F_{30}/F_0)_{NC} < 1.2$
340 indicates the negative result.

341 For the lateral flow readout, a 100 μl-reaction mixture was incubated in an
342 Eppendorf tube at 37 °C for 30 min. Then, the HybriDetect strip (Milenia Biotec,
343 Giessen, Germany) was placed into the Eppendorf tube, and the C-line and/or T-line
344 were visualized and stabilized in ~2 min. The relative greyness of the T-line (G) was
345 quantified using ImageJ. In this study, $G_{Sample} / G_{NC} \geq 1.5$ indicates the positive result
346 while $G_{Sample} / G_{NC} < 1.5$ indicates the negative result. Due to the incomplete
347 digestion of FB-ssDNA, some positive test results displayed two lines (T-line and
348 C-line) on the strips.

349

350 **CRISPR *cis*-cleavage assay**

351 Upon detection of the targeted sites, the CRISPR-Cas12a system is capable to
352 *cis*-cleave the dsDNA template into two short fragments, the activity of which was
353 determined by sodium dodecyl sulfate-polyacrylamide gel electrophoresis
354 (SDS-PAGE). After a 30-min incubation of the CRISPR reaction mixture as
355 described above, the mixture was denatured at 95 °C for 5 min. Then, it was loaded
356 into an 8% SDS-PAGE for 45 min at 150 V. The gel was stained with GelRed
357 (Biotium, CA, USA) and analyzed by Image J.

358

359 **Specificity of RRCd assay**

360 To test if RRCd could discriminate SARS-CoV-2 from the phylogenetically
361 related viruses, DNA fragments containing selected regions of *N* gene of SARS-CoV
362 (NC_004718.3), MERS CoV (NC_019843.3), and H1N1 (NC_026433.1,
363 NC_026434.1) were synthesized from Sangon Biotech (**Supplementary Table 2**),

and then cloned into a T7 promoter expression plasmid to be used as the templates for IVT of viral RNAs, respectively. The transcribed RNAs were detected using crRNA-SARS-CoV2 *N* by the RRCd assay as described above.

Building a standard curve to determine the relationship between viral copy numbers and the C_t values

The pseudovirus SARS-CoV-2 ab II EMNS S-MT and SARS-CoV-2-MT-B.1.617.2. (**Supplementary Table 3**) were purchased from FUBIO, Nanjing, China. To establish the correlation between viral copy numbers and the C_t values of SARS-CoV-2, we built a standard curve using a gradient dilution (1×10^5, 1×10^4, 1×10^3, 1×10^2, 10 and 5 RNA copies per reaction) of SARS-CoV-2 ab II EMNS S-MT. The C_t values of the samples were determined by targeting *N* gene and *ORF1ab* gene with RT-qPCR as mentioned above. Results were plotted against the viral copy numbers yielding a linear relationship.

Limit of detection (LoD) of RRCd assay

To determinate the detection limits of RRCd assay for different SARS-CoV-2 variants (*E* gene, T478, K478, N501 and Y501 in *S* gene), nine serial dilutions (1×10^7, 1×10^6, 1×10^5, 1×10^4, 1×10^3, 1×10^2, 10 and 5 copies per reaction) of SARS-CoV-2 pseudovirus RNAs were used and their fluorescence-based and lateral-flow readouts were analyzed as described above. For the dilutions (1×10^7, 1×10^6, 1×10^5, 1×10^4, 1×10^3 and 1×10^2 copies per reaction), at least three independent experiments were performed, while for the dilutions with 10 and 5 copies per reaction, at least five independent experiments were conducted. RNase-free water was used as the negative control.

389

390 **Whole-genome sequencing of clinical samples**

391 To determine the lineages of the RT-qPCR-verified positive clinical samples,
392 whole-genome sequencing of SARS-CoV-2 cDNA was conducted by Illumina
393 Next-generation sequencing. The first-strand cDNA of SARS-CoV-2 RNA was
394 generated using the SuperScript IV First-Strand Synthesis System (Cat# 18091050,
395 Thermo Fisher Scientific). The corresponding libraries were constructed using the
396 cDNAs with the ARTIC SARS-CoV-2 amplification protocol (as described in
397 https://artic.network/ncov-2019). Paired-end 150 bp sequencing was performed for
398 each library on Illumina X-10. Genome assembly was done using CLC Genomics
399 Workbench (http://www.clcbio.com/products/clcgenomics-workbench/) (Liu and Di
400 2020). The Phylogenetic Assignment of Named Global Outbreak Lineages
401 (PANGOLIN) (https://virological.org/t/pangolin-web-application-release/482) (Lam
402 et al. 2020) and the NextClade (https://clades.nextstrain.org/) (Hadfield et al. 2018)
403 were used for lineage classification and clade classification, respectively. All the *S*
404 gene from the positive clinical samples used in this study were re-sequenced by
405 Sanger method.

406

407 **Optimization of RRCd assay**

408 To optimize the RT reaction, we first investigated the effects of different RNA
409 input (1, 5, or 10 μl) on the detection sensitivity of RRCd. RNA was extracted from
410 a positive clinical sample (C_t = 30) as described above and the SARS-CoV-2 *E* gene
411 was used as the test target.

412 RNase H is an endoribonuclease that specifically hydrolyzes the RNA-DNA
413 hybrids(Qian et al. 2020), while T4 gene 32 protein is known to increase the

efficiency of reverse transcriptase(Villalva et al. 2001) and Bsu DNA polymerase has the strand displacement DNA synthesis activity(Piepenburg et al. 2006). To evaluate the effects of these enzymes on RT-RPA efficiency, a basic RT reaction mixture was prepared as described above with or without the addition of 250 U RNase H (Cat# M0297S, New England Biolabs), 16.5 μM T4 gene 32 protein (Cat# M0300L, New England Biolabs) or 0.25 U Bsu DNA polymerase (Cat# M0330S, New England Biolabs), respectively.

The corresponding RT products were used as inputs to the RPA assay and subsequent products were analyzed by fluorescence based CRISPR assay as described above. Finally, a 20 μl volume-optimized RT reaction mixture was obtained as below: 1 × RT buffer, 10 μl template RNA, 200 U RevertAid reverse transcriptase (Thermo Scientific), 1.25 μM RT-RPA forward and reverse primer mix, 1 mM dNTP mix, 20 U RNase inhibitor (Thermo Scientific), 250 U RNase H (New England Biolabs) and 16.5 μM T4 gene 32 protein (New England Biolabs).

For screening of an optimal RPA kit, four RPA assay kits were compared under the same conditions, including Amp-Qitian kit (Qitian gene Biotech, Wuxi, China), Amp-Future kit (Amp-Future, Weifang, China), TwistAmp Baic kit (TwistDx, Cambridge, UK), and Amp-Yizhi Kit (Yizhi Biotech, Shenzhen, China). Briefly, 10 μl RT product was transferred into a 50 μl volume basic RPA reaction mixture using these four kits, respectively, which contains 29.5 μl rehydration buffer, one freeze-dried RPA reaction pellet, 0.5 μM RT-RPA forward and reverse primer mix, and 14 mM MgOAc (last added to initiate the reaction). The RPA reaction mixture was incubated at 37 °C for 15 min. RNase-free water was used as the negative control.

To investigate the possible effects of T4 gene 32 protein and Bsu DNA

polymerase on RPA reaction, basic RPA reaction mixture was prepared as described above with or without the addition of 16.5 μM T4 gene 32 protein (Cat# M0300L, New England Biolabs) or 0.25U Bsu DNA polymerase (Cat# M0330S, New England Biolabs).

The RT-RPA products were analyzed by fluorescence based CRISPR assay as described above. Finally, a 50 μl volume-optimized RPA reaction mixture was obtained as below: 29.5 μl rehydration buffer (TwistDx), one freeze-dried RPA reaction pellet (TwistDx), 10 μl RT product, 0.5 μM RT-RPA forward and reverse primer mix, 16.5 μM T4 gene 32 protein (Cat# M0300L, New England Biolabs) and 14 mM MgOAc.

To determine if the CRISPR reaction has a higher efficiency using manganese rather than magnesium, as described before(Li et al. 2020). The fluorescence-based CRISPR assay was used to quantify the results as described above, with 10 mM $MnCl_2$ or $MgCl_2$ in the basic CRISPR reaction mixture.

Furthermore, the optimal concentrations of FQ-ssDNA and FB-ssDNA probes were determined within the basic CRISPR reaction mixture. The FQ-ssDNA probe (10, 15, or 20 nM) and FB-ssDNA probe (0.5, 5, 25, 50, 125, 200, 500, 1000, or 2000 nM) were used in the CRISPR reaction, and the corresponding reaction fluorescence intensities and lateral-flow readouts were recorded as described above, respectively.

Finally, a 100 μl volume-optimized CRISPR reaction mixture was obtained as below: 1 × *Lba*Cas12a buffer (Cat# M0653T, New England Biolabs), 5 μl RT-RPA product, 0.2 μM *Lba*Cas12a (Cat# M0653T, New England Biolabs), 0.6 μM crRNA, 10 μM $MgCl_2$, and 20 nM FAM-BHQ1 ssDNA probe for the fluorescence-based detection, or 200 nM FTIC-Biotin ssDNA probe for the lateral flow-based detection.

464

465 **Comparison of the one-step and two-step RT-RPA**

466 The amplification efficiency from the one-step and two-step RT-RPA was
467 compared by using *E* gene as the detection target. The two-step RT-RPA was
468 conducted using the optimized RT-RPA mixtures as described above, while the
469 one-step RT-RPA was performed by adding all the reaction reagents at once and
470 incubated at 37 °C for 30 min. The 50 µl-reaction mixture of the one-step RT-RPA
471 contains 29.5 µl rehydration buffer, 10 µl RNA template, one freeze-dried Twist RPA
472 reaction pellet, 2.5 µM RT-RPA forward and reverse primer mix, 0.4 mM dNTP mix,
473 200 U RevertAid reverse transcriptase, 6.6 µM T4 gene 32 protein, 100 U RNase H,
474 10 U RNase inhibitor, and 14 mM MgOAc. The RT-RPA products were loaded into
475 8% PAGE gel and the relative greyness of sample bands was quantified using
476 ImageJ.

477

478 **Validation of RRCd in detection and discrimination of clinical samples**

479 To evaluate the performance of RRCd on SARS-CoV-2 clinical samples, a
480 total of 204 swabs were collected at SITHC from March 3rd and to October 29th 2021
481 and were used to perform the RRCd assay. Both lateral-flow and fluorescence-based
482 readouts were recorded. A total of 96 clinical samples were used to detect
483 SARS-CoV-2 by targeting *E* gene and *S* gene, and a total of 108 clinical samples
484 were used to detect and discriminate the SARS-CoV-2 VOCs by targeting *S* gene
485 501 or 478. The RRCd results were analyzed and compared with the results of
486 RT-qPCR and genome sequencing.

487

488 **RRCd using the directly released RNA**

Viral RNAs from SARS-CoV-2 pseudovirus and clinical samples were released directly by a Sample release reagent kit (Sansure Biotech, Changsha, China) according to the manufacturer's instructions with minor modifications. The swab storage solution and the sample release reagent were mixed in a ratio of 1:1 and incubated at 37 °C for 5 min before subsequent assays.

Statistical analysis

Data were represented as mean ± S.D. from three independent experiments otherwise indicated. Statistical significances were analyzed by using the R (version 4.1.1). Unpaired one-tailed *t*-test was applied to investigate the differences between groups assuming P value < 0.05 as significant.

Acknowledgements

We are grateful to Prof. Xian-En Zhang for generously providing the pseudovirus, and Prof. Hang Dai and Dr. Xiaonan Yang for constructive discussion on this project. This study was supported by the National Key R&D Program of China (2019YFA0904003, 2020YFA0909100), the Strategic Priority Research Program of the Chinese Academy of Sciences, China (XDB38020300), the Guangdong Basic and Applied Basic Research Foundation (2021A1515012511), and the General Administration of Customs Project (2020HK003).

Author contributions

G.P.Z., Z.G.T. and W.Z. conceived and designed the study. G.T., Z.Z., W.T. and F.L. performed the experiments and analyzed data. All authors contributed to writing and editing of the manuscript. W.Z. supervised the research.

Competing interests

G.Y.T., W.T., G.P.Z. and W.Z. are co-inventors on patent applications filed by Shenzhen Institutes of Advanced Technology relating to the work in this manuscript. The remaining authors declare no conflict of interest.

References

Broughton, J. P., X. Deng, G. Yu, C. L. Fasching, V. Servellita, J. Singh, X. Miao, J. A. Streithorst, A. Granados, A. Sotomayor-Gonzalez, K. Zorn, A. Gopez, E. Hsu, W. Gu, S. Miller, C. Y. Pan, H. Guevara, D. A. Wadford, J. S. Chen, and C. Y. Chiu. 2020. "CRISPR-Cas12-based detection of SARS-CoV-2." *Nat Biotechnol* 38 (7):870-874. doi: 10.1038/s41587-020-0513-4.

Buch, J., K. Roomp, G. Bach, L. Steinbruck, M. Beer, V. Gregory, N. Komadina, Y. Lan, I. Monne, C. Smith, S. Fujisaki, P. Bogner, and T. Lengauer. 2011. "GISAID - a global initiative on sharing all influenza data." *Influenza and Other Respiratory Viruses* 5:419-419.

Chen, J. S., E. Ma, L. B. Harrington, M. Da Costa, X. Tian, J. M. Palefsky, and J. A. Doudna. 2018. "CRISPR-Cas12a target binding unleashes indiscriminate single-stranded DNase activity." *Science* 360 (6387):436-439. doi: 10.1126/science.aar6245.

Crits-Christoph, A., R. S. Kantor, M. R. Olm, O. N. Whitney, B. Al-Shayeb, Y. C. Lou, A. Flamholz, L. C. Kennedy, H. Greenwald, A. Hinkle, J. Hetzel, S. Spitzer, J. Koble, A. Tan, F. Hyde, G. Schroth, S. Kuersten, J. F. Banfield, and K. L. Nelson. 2021. "Genome Sequencing of Sewage Detects Regionally Prevalent SARS-CoV-2 Variants." *Mbio* 12 (1). doi: ARTN e02703-2010.1128/mBio.02703-20.

de Puig, H., R. A. Lee, D. Najjar, X. Tan, L. R. Soeknsen, N. M. Angenent-Mari, N. M. Donghia, N. E. Weckman, A. Ory, C. F. Ng, P. Q. Nguyen, A. S. Mao, T. C. Ferrante, G. Lansberry, H. Sallum, J. Niemi, and J. J. Collins. 2021. "Minimally instrumented SHERLOCK (miSHERLOCK) for CRISPR-based point-of-care diagnosis of SARS-CoV-2 and emerging variants." *Sci Adv* 7 (32). doi: 10.1126/sciadv.abh2944.

Ding, X., K. Yin, Z. Li, R. V. Lalla, E. Ballesteros, M. M. Sfeir, and C. Liu. 2020. "Ultrasensitive and visual detection of SARS-CoV-2 using all-in-one dual CRISPR-Cas12a assay." *Nat Commun* 11 (1):4711. doi: 10.1038/s41467-020-18575-6.

Fozouni, P., S. Son, M. Diaz de Leon Derby, G. J. Knott, C. N. Gray, M. V. D'Ambrosio, C. Zhao, N. A. Switz, G. R. Kumar, S. I. Stephens, D. Boehm, C. L. Tsou, J. Shu, A. Bhuiya, M. Armstrong, A. R. Harris, P. Y. Chen, J. M. Osterloh, A. Meyer-Franke, B. Joehnk, K. Walcott, A. Sil, C. Langelier, K. S. Pollard, E. D. Crawford, A. S. Puschnik, M. Phelps, A. Kistler, J. L. DeRisi, J. A. Doudna, D. A. Fletcher, and M. Ott. 2021. "Amplification-free detection of SARS-CoV-2 with CRISPR-Cas13a and mobile phone microscopy." *Cell* 184 (2):323-333 e9. doi: 10.1016/j.cell.2020.12.001.

Hadfield, J., C. Megill, S. M. Bell, J. Huddleston, B. Potter, C. Callender, P. Sagulenko, T. Bedford,

554 and R. A. Neher. 2018. "Nextstrain: real-time tracking of pathogen evolution."
555 *Bioinformatics* 34 (23):4121-4123. doi: 10.1093/bioinformatics/bty407.
556 Joung, J., A. Ladha, M. Saito, N. G. Kim, A. E. Woolley, M. Segel, R. P. J. Barretto, A. Ranu, R. K.
557 Macrae, G. Faure, E. I. Ioannidi, R. N. Krajeski, R. Bruneau, M. W. Huang, X. G. Yu, J. Z.
558 Li, B. D. Walker, D. T. Hung, A. L. Greninger, K. R. Jerome, J. S. Gootenberg, O. O.
559 Abudayyeh, and F. Zhang. 2020. "Detection of SARS-CoV-2 with SHERLOCK One-Pot
560 Testing." *N Engl J Med* 383 (15):1492-1494. doi: 10.1056/NEJMc2026172.
561 Julia L. Mullen, Ginger Tsueng, Alaa Abdel Latif, Manar Alkuzweny, Marco Cano, Emily Haag, Jerry
562 Zhou, Mark Zeller, Emory Hufbauer, Nate Matteson, Kristian G. Andersen, Chunlei Wu,
563 Andrew I. Su, Karthik Gangavarapu, Laura D. Hughes and Center for Viral Systems Biology.
564 2021. Outbreak.info. https://outbreak.info/situation-reports."
565 Kumar, M., S. Gulati, A. H. Ansari, R. Phutela, S. Acharya, M. Azhar, J. Murthy, P. Kathpalia, A.
566 Kanakan, R. Maurya, J. S. Vasudevan, A. S, R. Pandey, S. Maiti, and D. Chakraborty. 2021.
567 "FnCas9-based CRISPR diagnostic for rapid and accurate detection of major SARS-CoV-2
568 variants on a paper strip." *Elife* 10. doi: 10.7554/eLife.67130.
569 Kumar, S., T. S. Thambiraja, K. Karuppanan, and G. Subramaniam. 2022. "Omicron and Delta variant
570 of SARS-CoV-2: A comparative computational study of spike protein." *J Med Virol* 94
571 (4):1641-1649. doi: 10.1002/jmv.27526.
572 Lam, T. T., N. Jia, Y. W. Zhang, M. H. Shum, J. F. Jiang, H. C. Zhu, Y. G. Tong, Y. X. Shi, X. B. Ni, Y.
573 S. Liao, W. J. Li, B. G. Jiang, W. Wei, T. T. Yuan, K. Zheng, X. M. Cui, J. Li, G. Q. Pei, X.
574 Qiang, W. Y. Cheung, L. F. Li, F. F. Sun, S. Qin, J. C. Huang, G. M. Leung, E. C. Holmes, Y.
575 L. Hu, Y. Guan, and W. C. Cao. 2020. "Identifying SARS-CoV-2-related coronaviruses in
576 Malayan pangolins." *Nature* 583 (7815):282-285. doi: 10.1038/s41586-020-2169-0.
577 Li, B., J. Yan, Y. Zhang, W. Li, C. Zeng, W. Zhao, X. Hou, C. Zhang, and Y. Dong. 2020.
578 "CRISPR-Cas12a Possesses Unconventional DNase Activity that Can Be Inactivated by
579 Synthetic Oligonucleotides." *Mol Ther Nucleic Acids* 19:1043-1052. doi:
580 10.1016/j.omtn.2019.12.038.
581 Li, S. Y., Q. X. Cheng, J. K. Liu, X. Q. Nie, G. P. Zhao, and J. Wang. 2018. "CRISPR-Cas12a has
582 both cis- and trans-cleavage activities on single-stranded DNA." *Cell Res* 28 (4):491-493.
583 doi: 10.1038/s41422-018-0022-x.
584 Li, S. Y., Q. X. Cheng, J. M. Wang, X. Y. Li, Z. L. Zhang, S. Gao, R. B. Cao, G. P. Zhao, and J. Wang.
585 2018. "CRISPR-Cas12a-assisted nucleic acid detection." *Cell Discov* 4:20. doi:
586 10.1038/s41421-018-0028-z.
587 Liu, C. H., and Y. P. Di. 2020. "Analysis of RNA Sequencing Data Using CLC Genomics
588 Workbench." *Methods Mol Biol* 2102:61-113. doi: 10.1007/978-1-0716-0223-2_4.
589 Liu, Y., J. Liu, K. S. Plante, J. A. Plante, X. Xie, X. Zhang, Z. Ku, Z. An, D. Scharton, C. Schindewolf,
590 S. G. Widen, V. D. Menachery, P. Y. Shi, and S. C. Weaver. 2022. "The N501Y spike
591 substitution enhances SARS-CoV-2 infection and transmission." *Nature* 602
592 (7896):294-299. doi: 10.1038/s41586-021-04245-0.
593 Lobato, I. M., and C. K. O'Sullivan. 2018. "Recombinase polymerase amplification: Basics,
594 applications and recent advances." *Trends Analyt Chem* 98:19-35. doi:
595 10.1016/j.trac.2017.10.015.
596 Meng, B., S. A. Kemp, G. Papa, R. Datir, Iatm Ferreira, S. Marelli, W. T. Harvey, S. Lytras, A.
597 Mohamed, G. Gallo, N. Thakur, D. A. Collier, P. Mlcochova, Covid- Genomics UK

598 Consortium, L. M. Duncan, A. M. Carabelli, J. C. Kenyon, A. M. Lever, A. De Marco, C.
599 Saliba, K. Culap, E. Cameroni, N. J. Matheson, L. Piccoli, D. Corti, L. C. James, D. L.
600 Robertson, D. Bailey, and R. K. Gupta. 2021. "Recurrent emergence of SARS-CoV-2 spike
601 deletion H69/V70 and its role in the Alpha variant B.1.1.7." *Cell Rep* 35 (13):109292. doi:
602 10.1016/j.celrep.2021.109292.
603 Munnink, B. B. O., N. Worp, D. F. Nieuwenhuijse, R. S. Sikkema, B. Haagmans, R. A. M. Fouchier,
604 and M. Koopmans. 2021. "The next phase of SARS-CoV-2 surveillance: real-time molecular
605 epidemiology." *Nature Medicine* 27 (9):1518-1524. doi: 10.1038/s41591-021-01472-w.
606 Nyberg, T., N. M. Ferguson, S. G. Nash, H. H. Webster, S. Flaxman, N. Andrews, W. Hinsley, J. L.
607 Bernal, M. Kall, S. Bhatt, P. Blomquist, A. Zaidi, E. Volz, N. A. Aziz, K. Harman, S. Funk, S.
608 Abbott, Covid- Genomics UK consortium, R. Hope, A. Charlett, M. Chand, A. C. Ghani, S.
609 R. Seaman, G. Dabrera, D. De Angelis, A. M. Presanis, and S. Thelwall. 2022. "Comparative
610 analysis of the risks of hospitalisation and death associated with SARS-CoV-2 omicron
611 (B.1.1.529) and delta (B.1.617.2) variants in England: a cohort study." *Lancet*. doi:
612 10.1016/S0140-6736(22)00462-7.
613 Oude Munnink, B. B., N. Worp, D. F. Nieuwenhuijse, R. S. Sikkema, B. Haagmans, R. A. M.
614 Fouchier, and M. Koopmans. 2021. "The next phase of SARS-CoV-2 surveillance: real-time
615 molecular epidemiology." *Nat Med* 27 (9):1518-1524. doi: 10.1038/s41591-021-01472-w.
616 Patchsung, M., K. Jantarug, A. Pattama, K. Aphicho, S. Suraritdechachai, P. Meesawat, K. Sappakhaw,
617 N. Leelahakorn, T. Ruenkam, T. Wongsatit, N. Athipanyasilp, B. Eiamthong, B.
618 Lakkanasirorat, T. Phoodokmai, N. Niljianskul, D. Pakotiprapha, S. Chanarat, A. Homchan,
619 R. Tinikul, P. Kamutira, K. Phiwkaow, S. Soithongcharoen, C. Kantiwiriyawanitch, V.
620 Pongsupasa, D. Trisrivirat, J. Jaroensuk, T. Wongnate, S. Maenpuen, P. Chaiyen, S.
621 Kamnerdnakta, J. Swangsri, S. Chuthapisith, Y. Sirivatanauksorn, C. Chaimayo, R. Sutthent,
622 W. Kantakamalakul, J. Joung, A. Ladha, X. Jin, J. S. Gootenberg, O. O. Abudayyeh, F.
623 Zhang, N. Horthongkham, and C. Uttamapinant. 2020. "Clinical validation of a Cas13-based
624 assay for the detection of SARS-CoV-2 RNA." *Nat Biomed Eng* 4 (12):1140-1149. doi:
625 10.1038/s41551-020-00603-x.
626 Peto, T., and Uk Covid- Lateral Flow Oversight Team. 2021. "COVID-19: Rapid antigen detection for
627 SARS-CoV-2 by lateral flow assay: A national systematic evaluation of sensitivity and
628 specificity for mass-testing." *EClinicalMedicine* 36:100924. doi:
629 10.1016/j.eclinm.2021.100924.
630 Piepenburg, O., C. H. Williams, D. L. Stemple, and N. A. Armes. 2006. "DNA detection using
631 recombination proteins." *Plos Biology* 4 (7):1115-1121. doi: ARTN
632 e20410.1371/journal.pbio.0040204.
633 Qian, J., S. A. Boswell, C. Chidley, Z. X. Lu, M. E. Pettit, B. L. Gaudio, J. M. Fajnzylber, R. T.
634 Ingram, R. H. Ward, J. Z. Li, and M. Springer. 2020. "An enhanced isothermal amplification
635 assay for viral detection." *Nat Commun* 11 (1):5920. doi: 10.1038/s41467-020-19258-y.
636 Tao, K., P. L. Tzou, J. Nouhin, R. K. Gupta, T. de Oliveira, S. L. Kosakovsky Pond, D. Fera, and R. W.
637 Shafer. 2021. "The biological and clinical significance of emerging SARS-CoV-2 variants."
638 *Nat Rev Genet* 22 (12):757-773. doi: 10.1038/s41576-021-00408-x.
639 Tegally, H., E. Wilkinson, M. Giovanetti, A. Iranzadeh, V. Fonseca, J. Giandhari, D. Doolabh, S.
640 Pillay, E. J. San, N. Msomi, K. Mlisana, A. von Gottberg, S. Walaza, M. Allam, A. Ismail, T.
641 Mohale, A. J. Glass, S. Engelbrecht, G. Van Zyl, W. Preiser, F. Petruccione, A. Sigal, D.

642 Hardie, G. Marais, N. Y. Hsiao, S. Korsman, M. A. Davies, L. Tyers, I. Mudau, D. York, C.
643 Maslo, D. Goedhals, S. Abrahams, O. Laguda-Akingba, A. Alisoltani-Dehkordi, A. Godzik,
644 C. K. Wibmer, B. T. Sewell, J. Lourenco, L. C. J. Alcantara, S. L. Kosakovsky Pond, S.
645 Weaver, D. Martin, R. J. Lessells, J. N. Bhiman, C. Williamson, and T. de Oliveira. 2021.
646 "Detection of a SARS-CoV-2 variant of concern in South Africa." *Nature* 592
647 (7854):438-443. doi: 10.1038/s41586-021-03402-9.
648 Teng, F., L. Guo, T. Cui, X. G. Wang, K. Xu, Q. Gao, Q. Zhou, and W. Li. 2019. "CDetection:
649 CRISPR-Cas12b-based DNA detection with sub-attomolar sensitivity and single-base
650 specificity." *Genome Biol* 20 (1):132. doi: 10.1186/s13059-019-1742-z.
651 Villalva, C., C. Touriol, P. Seurat, P. Trempat, G. Delsol, and P. Brousset. 2001. "Increased yield of
652 PCR products by addition of T4 gene 32 protein to the SMART PCR cDNA synthesis
653 system." *Biotechniques* 31 (1):81-3, 86. doi: 10.2144/01311st04.
654 Vogels, C. B. F., M. I. Breban, I. M. Ott, T. Alpert, M. E. Petrone, A. E. Watkins, C. C. Kalinich, R.
655 Earnest, J. E. Rothman, J. G. de Jesus, I. M. Claro, G. M. Ferreira, M. A. E. Crispim, L.
656 Singh, H. Tegally, U. J. Anyaneji, E. B. Hodcroft, C. E. Mason, G. Khullar, J. Metti, J. T.
657 Dudley, M. J. MacKay, M. Nash, J. H. Wang, C. Liu, P. Hui, S. Murphy, C. Neal, E. Laszlo,
658 M. L. Landry, A. Muyombwe, R. Downing, J. Razeq, T. de Oliveira, N. R. Faria, E. C.
659 Sabino, R. A. Neher, J. R. Fauver, N. D. Grubaugh, Brazil-UK CADDE Genomic Network,
660 and Network Genomic Surveillance South. 2021. "Multiplex qPCR discriminates variants of
661 concern to enhance global surveillance of SARS-CoV-2." *Plos Biology* 19 (5). doi: ARTN
662 e300123610.1371/journal.pbio.3001236.
663 Wang, Y., Y. Zhang, J. Chen, M. Wang, T. Zhang, W. Luo, Y. Li, Y. Wu, B. Zeng, K. Zhang, R. Deng,
664 and W. Li. 2021. "Detection of SARS-CoV-2 and Its Mutated Variants via
665 CRISPR-Cas13-Based Transcription Amplification." *Anal Chem* 93 (7):3393-3402. doi:
666 10.1021/acs.analchem.0c04303.
667

668 **Table 1. Comparison of RRCd with DETECTR and SHERLOCK for the**
669 **SARS-CoV-2 detection.**

	RRCd	**DETECTR** (Broughton et al. 2020)	**SHERLOCK** (Patchsung et al. 2020)
Target genes	*S*, *E* and *N*	*E* and *N*	*Orf1ab*, *S* and *N*
Assay procedures	RT-RPA (37 °C, 30 min); Cas12 reaction (37 °C, 30 min); Lateral flow strip (room temperature, 2 min)	RT-LAMP (62 °C, 20-30 min); Cas12 reaction (37 °C, 10 min); Lateral flow strip (room temperature, 2 min)	RT-RPA (42 °C, 25 min); T7 transcription and Cas13 reaction (37 °C, 30 min); Lateral flow strip (room temperature, 2 min)
Assay time	~ 60 min	~ 45 min	~ 60 min
LoD	10	20	42
Specificity	SNP and small deletion	NA	NA
RNA purification dependence	No	Yes	Yes

670 LoD, limit of detection (copies per reaction); NA, not applicable.

671 **Table 2. Predictive agreements of RRCd in detection of clinical samples.**

	RRCd results	RT-qPCR-verified positive samples		RT-qPCR-verified negative samples
		$C_t < 33$	$C_t \geq 33$	
Fluorescence-based readout	Positive	84 (true positive)	24 (true positive)	0 (false positive)
	Negative	1 (false negative)	13 (false negative)	82 (true negative)
	Total	85	37	82
	PPA/NPA	99%	65%	100%
	Total PPA/NPA	89%		100%
Lateral-flow readout	Positive	84 (true positive)	23 (true positive)	0 (false positive)
	Negative	1 (false negative)	14 (false negative)	82 (true negative)
	Total	85	37	82
	PPA/NPA	99%	62%	100%
	Total PPA/NPA	88%		100%

672 In total, 204 clinical samples including 122 positive samples and 82 negative
673 samples were analyzed by RRCd with both fluorescence-based and lateral-flow
674 readouts. PPA, positive predictive agreement; NPA, negative predictive agreement.

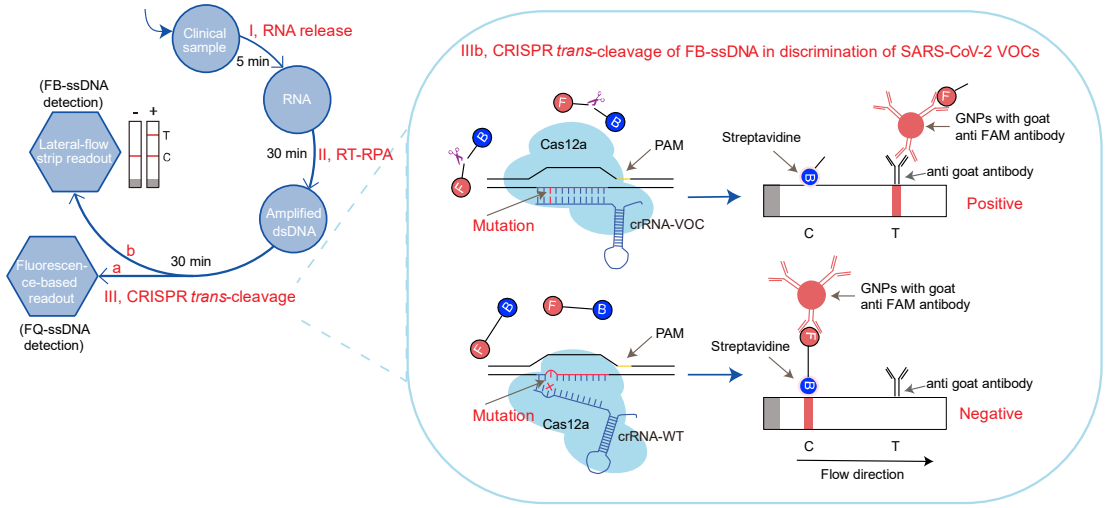

675

676 **Figure 1. Detection and discrimination of SARS-CoV-2 VOCs by RRCd.**

677 Schematic overview of RRCd workflow. (I) SARS-CoV-2 samples were released by
678 automatic extraction (~10 min) or using RNA release chemical agents without
679 extraction (~5 min). (II) The viral RNA was reverse transcribed into the dsDNA and
680 amplified by RPA. (III) Cas12a was guided to target the dsDNA by the specific
681 crRNA, thereby activated its *trans*-cleavage activity to the ssDNA probes in the
682 system. The results could be quantified by fluorescence detection of the cleaved
683 FQ-ssDNA (III a), or visualized by lateral-flow strip using the FB-ssDNA probe (III
684 b). RRCd in discrimination of SARS-CoV-2 VOCs with lateral-flow readout is
685 highlighted on the right panel. The target gene from SARS-CoV-2 variant was shown
686 as the template, and it was detected by either crRNA-VOC or crRNA-WT, leading to
687 the positive (upper right panel) or negative (lower right panel) test result,
688 respectively. dsDNA, double-strand DNA; ssDNA, single-strand DNA; FQ,
689 fluorophore (FAM)-quencher (BHQ1); FB, FITC-Biotin; PAM, protospacer adjacent
690 motif; VOC, variant of concern; WT, wild type; GNP, gold nanoparticle; gt, goat.

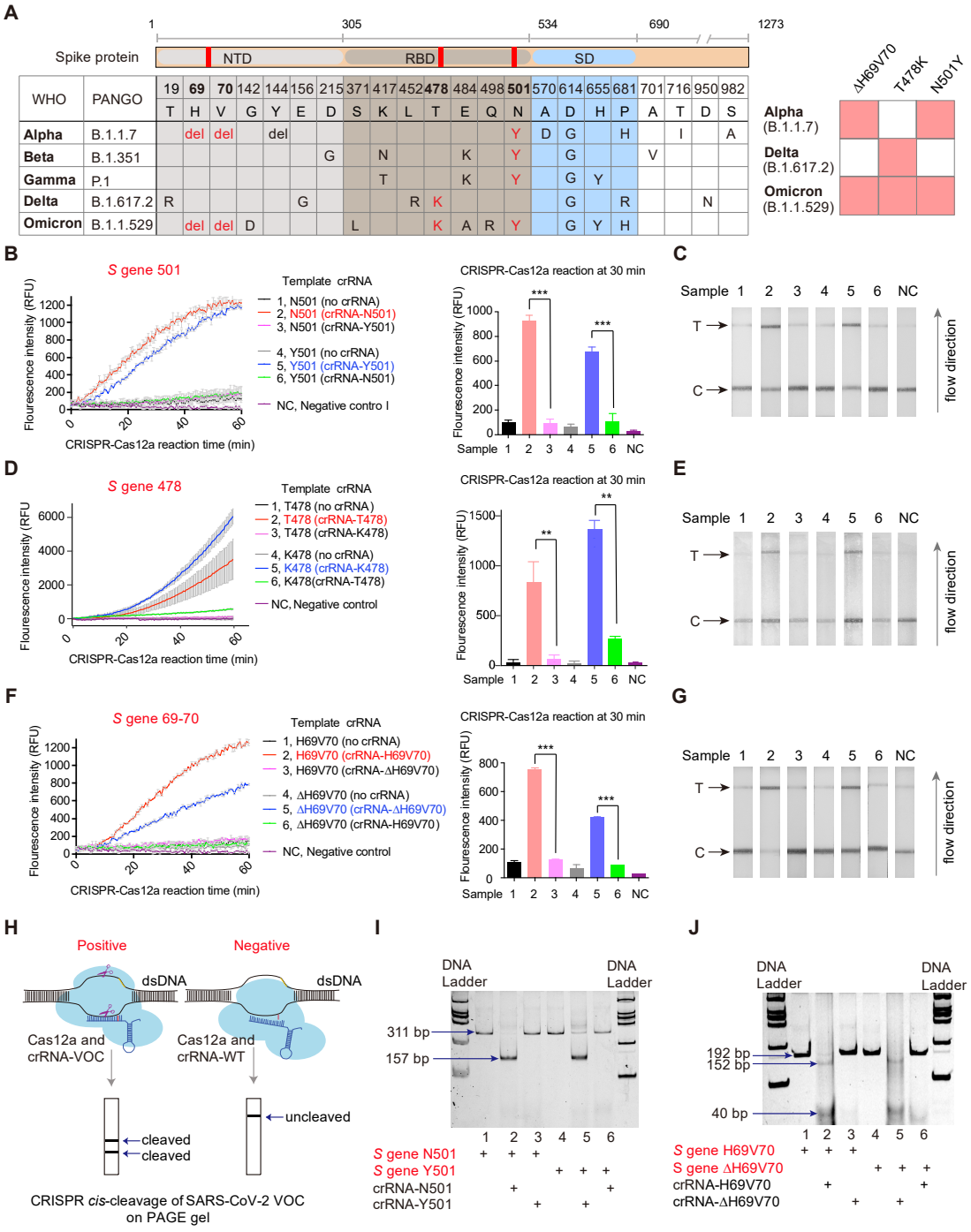

Figure 2. The specificity of RRCd in detection of SARS-CoV-2 VOCs. A. Representative changes of amino acids in the spike protein in different SARS-CoV-2 VOCs. Data came from Outbreak.info (https://outbreak.info/compare-lineages) (Julia L. Mullen 2021). The variations detected in this study are colored in red. A simple model is shown on the right panel. Del, deletion. **B**. Specificity analysis of RRCd in

detection of SARS-CoV-2 *S* gene 501, using fluorescence-based readouts. The dsDNA derived from pseudovirus *S* gene N501 or Y501 was incubated with Cas12a, FQ-ssDNA, and distinct crRNA at 37 °C, and the corresponding fluorescence signal was recorded over 60 min (left panel) and quantified at 30 min (right panel). Data are presented as the mean ± S.D. (n = 3). ***, $P < 0.01$ by student's *t* test. RNase-free water was used as the negative control (NC). RFU, relative fluorescence units. **C**. Specificity analysis of RRCd using lateral-flow readouts. The samples analyzed were the same as those in panel B. The reactions were conducted at 37 °C for 30 min before the mixtures were transferred onto the strips, using FB-ssDNA probe instead of FQ-ssDNA. The relative greyness (G) of strip bands was quantified using ImageJ. In this study, G_{Sample} / G_{NC} of the T band ≥ 1.5 indicates positive. **D, E**. Specificity analysis of RRCd in detection of SARS-CoV-2 *S* gene 478. **F, G**. Specificity analysis of RRCd in detection of SARS-CoV-2 *S* gene 69-70. **H**. Schematic of RRCd in detection of SARS-CoV-2 VOCs by Cas12a *cis*-cleavage activity. **I, J**. The specificity was demonstrated by PAGE analyses, using SARS-CoV-2 variants of N501Y and ΔH69-V70 as the examples.

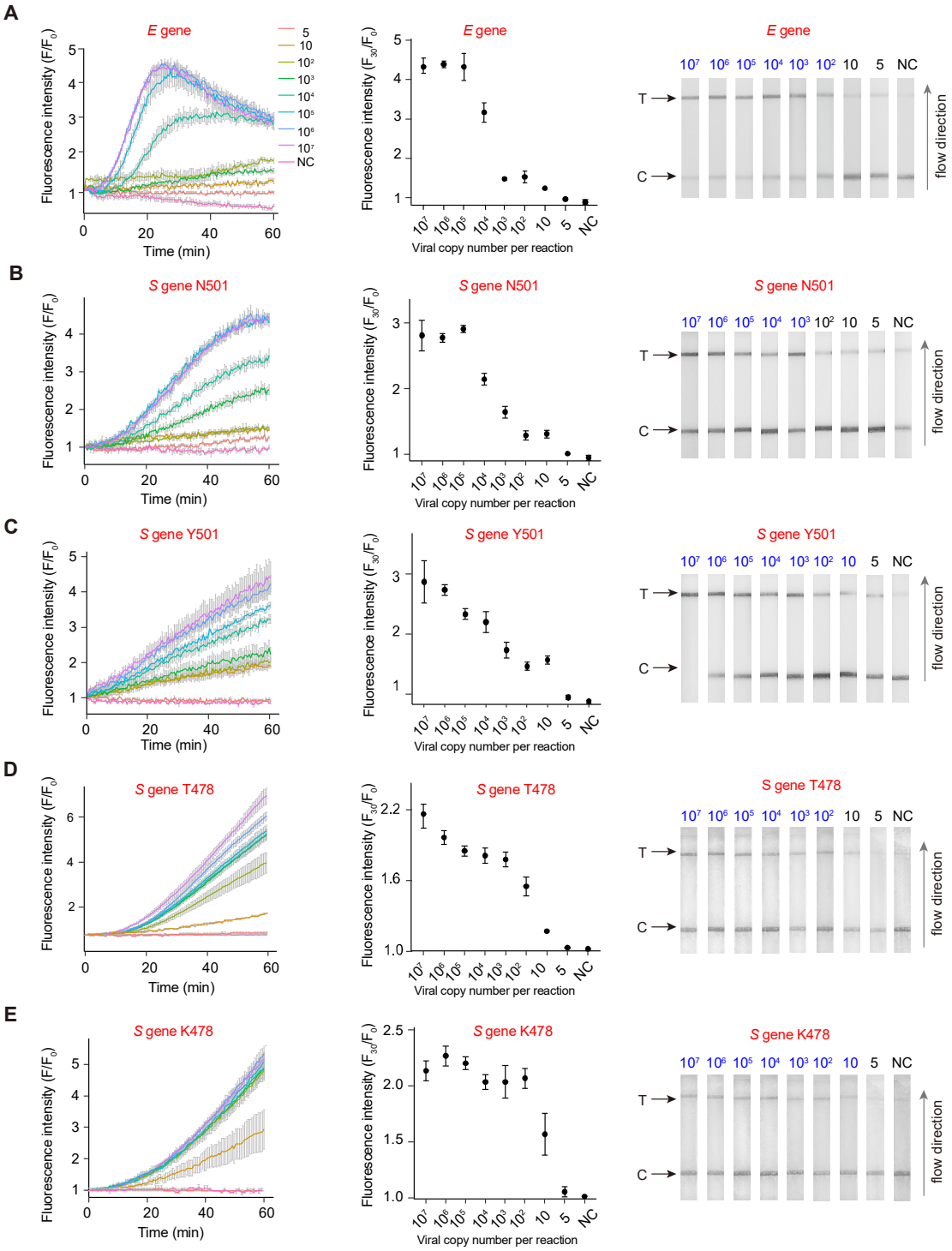

Figure 3. The detection limit of RRCd for SARS-CoV-2 VOCs. The detection limit of the targeted regions in VOCs were determined by using 10^7, 10^6, 10^5, 10^4, 10^3, 10^2, 10 and 5 copies of pseudovirus RNA per reaction, respectively. The dsDNA derived from the pseudovirus RNA was incubated with Cas12a, ssDNA probe, and crRNA at 37 °C for 60 min (fluorescence-based readouts) or 30 min (lateral-flow readouts),

719 respectively. The relative fluorescence intensity (F/F_0) was calculated as the
720 fluorescence signal versus the starting signal (left panel). Correspondingly, the
721 fluorescence signal at the 30 min-reaction was quantified (middle panel). The positive
722 samples of lateral-flow readouts (right panel) are indicated as blue by the T-line
723 quantification as described. Data are presented as mean ± S.D. from at least three
724 independent experiments. For the dilutions with 10 and 5 copies per reaction, at least
725 five independent experiments were conducted. **A**. LoD determination of RRCd for *E*
726 gene. **B-E**. LoD determinations of RRCd for N501 (B), Y501 (C), T478 (D) and K478
727 (E) in *S* gene, respectively. NC, negative control using the RNase-free water.

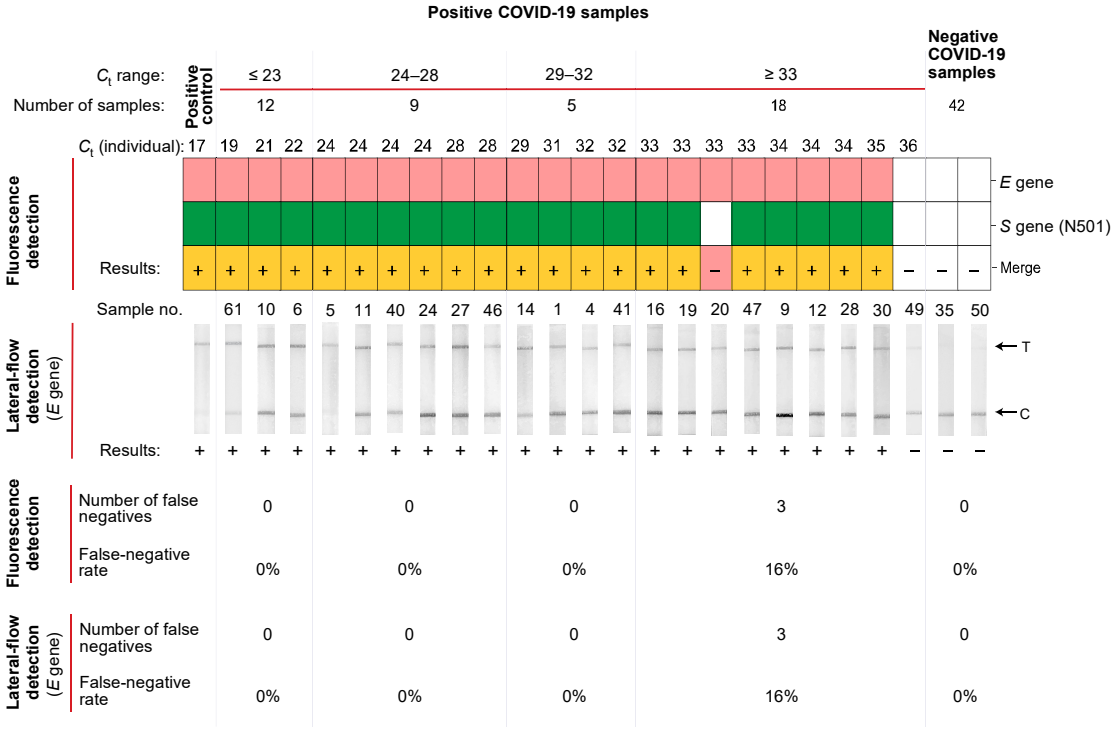

Figure 4. Validation of RRCd in detection of 96 RT-qPCR-verified clinical samples. Nasopharyngeal and salivary swabs were collected from 20th January to 10th April 2021 at Shanghai Customs, and a double-checked detection (*E* gene and *S* gene) was executed for them by RRCd. To minimize the cognitive bias, all information of the clinical samples was confidential to study staff before the detection. The results are displayed according to the C_t values of COVID-19 positive samples, and the total number of clinical samples in each C_t range are shown on the top of the panel. Representatives of fluorescence-based readouts and lateral-flow readouts of the positive samples as well as the negative samples are shown on the middle of the panel. Both *E* gene and *S* gene (N510) were used as the targeted sequences in fluorescence-based readouts. The light red and green indicate the positive detection results of *E* gene and *S* gene (N501), respectively, while the orange represents the

741 double-checked positive result. The white indicates the negative result. Only the
742 lateral-flow results of *E* gene are shown. +, positive; − , negative or indistinguishable.
743 The analyses of the detection results are shown as the number of false negatives and
744 the false-negative rate for each C_t range on the bottom of the panel. The SARS-CoV-2
745 pseudovirus was used as the positive control. The full dataset is shown in
746 Supplementary Figure 9.

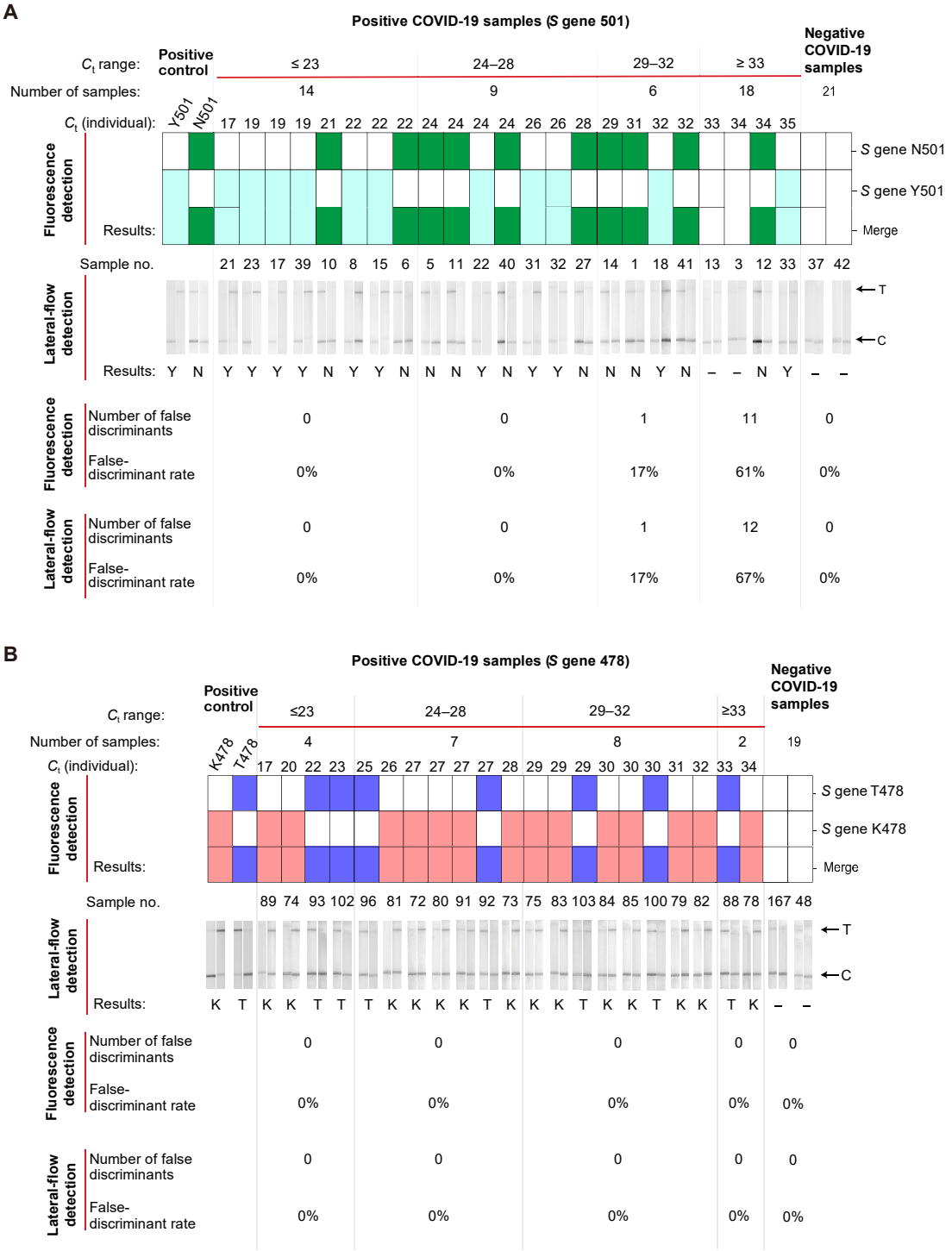

Figure 5. Validation of RRCd in detection and discrimination of 108 genome-sequencing-verified clinical samples. A. Discrimination of SARS-CoV-2 *S* gene 501 variants in clinical samples. The total number of clinical samples in each C_t range are shown on the top of the panel. In total, 47 positive samples (C_t range of 13-35) and 21 negative samples were detected. The *S* gene 501 variants were

753 discriminated by crRNA-N501 (green) and crRNA-Y501 (light blue) using
754 fluorescence-based readouts. In addition, the lateral-flow readouts are displayed in
755 the middle of the panel using crRNA-N501 (left) and crRNA-Y501 (right). N, N501;
756 Y, Y501; – , negative or indistinguishable. The analysis results are shown as the
757 number of false discriminants and the false-discriminant rate for each C_t range on the
758 bottom of the panel. **B**. Discrimination of SARS-CoV-2 *S* gene 478 variants in
759 clinical samples. In total, 21 positive samples (C_t range of 17-34) and 19 negative
760 samples were detected. The *S* gene 478 variants were discriminated by crRNA-T478
761 (blue) and crRNA-K478 (pink) by fluorescence readouts. The lateral-flow readouts
762 using crRNA_T478 (left) and crRNA_K478 (right) are displayed on the below. T,
763 T478; K, K478; – , negative or indistinguishable. The corresponding SARS-CoV-2
764 pseudoviruses were used as the positive controls. The full datasets for panel a and b
765 are shown in Supplementary Figure 10 and Supplementary Figure 11, respectively.